Relative Inclination Change Strategy for J_2-Perturbed Low-Thrust Transfers Between Circular Orbits

Adrian Barea*, Hodei Urrutxua† and Luis Cadarso‡
Universidad Rey Juan Carlos, Camino del Molino 5, 28942 Fuenlabrada, Spain

I. Introduction

The high concentration of space debris in particular zones of Low Earth Orbit (LEO) constitutes a considerable risk for the future of space operations. Specifically, it enhances the likelihood of a collision cascade phenomenon that would produce an uncontrollable generation of debris fragments [1]. Further studies have determined that the active removal of hazardous pieces of debris is necessary to achieve the stabilization of the number of objects within the zones of interest [2, 3]. In particular, it is expected that Active Debris Removal (ADR) missions will be able to remove several objects with a single servicing spacecraft. The use of low thrust propulsion constitutes a promising approach to ameliorate the substantial fuel requirements of such multi-target missions.

The most relevant candidate objects in LEO describe near-circular orbits. Thus, it is reasonable to consider transfers between circular orbits during the preliminary mission design. The classic Edelbaum approach [4] makes use of an averaged orbital dynamics to obtain an analytical solution of a minimum-time continuous-thrust transfer between two circular orbits. The Edelbaum solution was later reformulated as an optimal control problem [5] and extended to consider richer transfer models [6–8].

Moreover, such candidate objects are concentrated among different clusters of orbits with similar altitude and inclination. However, the objects within a cluster are, in general, arbitrarily spread in right ascension of the ascending node (RAAN). The usual strategy to traverse large RAAN differences during a transfer is to leverage the RAAN drift produced by the J_2 perturbation. The Cerf approach [9] uses a three-arc transfer (i.e., thrust-coast-thrust) in which the whole RAAN difference is overcome by the J_2 perturbation. Nevertheless, a better performance is achieved when the thrust carries out part of the RAAN change. The yaw switch steering approach (YSS) [10] considers it introducing the orbital position of the thrust reversal as a control variable.

The optimal target selection for ADR missions might require the consideration of pools of hundreds of relevant objects [11, 12], as well as the computation of a substantial amount of possible transfers. Hence the importance of developing fast and reliable evaluation methods for such transfers. The split Edelbaum strategy (SES) [9] is a simplification of the Cerf approach in which the thrust arcs are computed using the Edelbaum analytical solution. This results in a two-variable Nonlinear Programming problem (NLP). More recently, Shen [13] developed an explicit

*PhD Candidate, Aerospace Systems and Transport Research Group, Universidad Rey Juan Carlos. E-mail: adrian.barea@urjc.es
†Lecturer, Aerospace Systems and Transport Research Group, Universidad Rey Juan Carlos. E-mail: hodei.urrutxua@urjc.es
‡Associate Professor, Aerospace Systems and Transport Research Group, Universidad Rey Juan Carlos. E-mail: luis.cadarso@urjc.es

analytical approximation for the aforementioned three-arc transfers.

This work adds the effect of the J_2 perturbation to the Edelbaum approach, while considering the semimajor axis and relative inclination w.r.t. the target orbit (i.e., the angle of the current orbital plane with the target orbital plane) as the state variables. The optimal solution of this problem, albeit not analytical, only requires the determination of the initial value of the thrust yaw angle. Then, the final thrust arc of the SES approach is replaced with the proposed transfer. This results in a three-variable NLP problem. Additionally, two heuristic control laws of the proposed transfer are defined to further accelerate the resolution of the NLP problem. This methodology intends to exploit the RAAN change executed by the thrust to obtain potential Δv improvements, while maintaining a computational complexity similar to the one of the SES approach.

The remainder of this manuscript is organized as follows. Section II describes the resolution method of the continuous-thrust optimal control problem. Section III defines the three-arc transfer NLP problem. Section IV shows numerical experiments of the proposed methodology and provides a comparison with other relevant approaches. Finally, Section V summarizes the main conclusions of this work.

II. Continuous-thrust transfer

The problem at hand is to provide a time-optimal solution for a particular class of continuous-thrust transfers between circular orbits. Specifically, the proposed maneuver involves the application of tangential and out-of-plane thrust with the thrust yaw angle as the sole control variable. Moreover, the out-of-plane thrust is reversed when traversing the antinodes of the relative line of nodes w.r.t. the target orbit. Thus, the considered thrust produces changes in the semimajor axis as well as the relative inclination w.r.t. the target orbit. Additionally, the effect of the average J_2 perturbation in the RAAN is also considered.

A. Problem dynamics

The Edelbaum analytical solution is equally valid to represent inclination changes as well as changes of relative inclination w.r.t. the target orbit. The reason for it is that both kinds of maneuvers are geometrically identical, but seen from reference frames with different orientation. Namely, the usual equatorial coordinate system and a reference frame such that its XY plane is the target plane and its Z axis goes along the angular momentum of the target orbit, respectively. However, this is not true when considering the effect of the J_2 perturbation, as its contribution is not invariant under reference frame rotations. Thus, the dynamics equations that model the problem at hand are equivalent to the ones in [5] but with an additional term (γ) that quantifies the effect of the RAAN drift in the relative inclination:

$$\frac{\mathrm{d}a}{\mathrm{d}t} = 2\sqrt{\frac{a^3}{\mu}} f \cos(\beta) \tag{1}$$

$$\frac{\mathrm{d}i^*}{\mathrm{d}t} = \frac{2}{\pi}\sqrt{\frac{a}{\mu}} f \sin(\beta) + \gamma \tag{2}$$

where a and i^* are the semimajor axis and the relative inclination of the current orbit, respectively; f is the thrust acceleration; β is the thrust yaw angle; and μ is the gravitational parameter of the Earth.

The averaged RAAN drift produced by the J_2 perturbation for a circular orbit is:

$$\frac{\mathrm{d}\Omega}{\mathrm{d}t} = -\frac{3}{2} R_\oplus^2 J_2 \sqrt{\frac{\mu}{a^7}} \cos(i) \tag{3}$$

where Ω is the RAAN, $R_\oplus$ is the equatorial radius of the Earth, and J_2 is the coefficient of the spherical harmonic of degree 2 and order 0 of the Earth's gravity field.

Consequently, the determination of γ requires two tasks. On the one hand, the term $\cos(i)$ has to be redefined as a function of orbital parameters associated to the target orbit reference frame. On the other hand, the rate of change of Ω has to be turned into a rate of change of i^*.

Regarding the first task, the ascending nodes of the current (N) and target (N_f) orbits as well as the relative ascending node (N^*) constitute the spherical triangle shown in Figure 1, resulting in the following trigonometry laws:

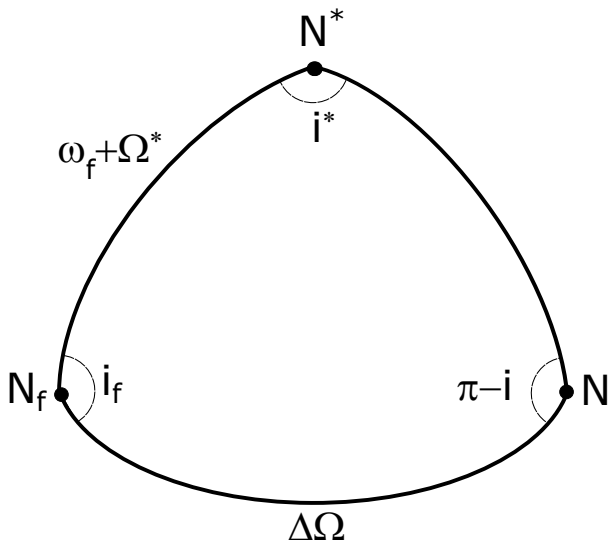

Fig. 1 Spherical triangle formed by ascending nodes.

$$\cos(i^*) = \cos(i)\cos(i_f) + \sin(i)\sin(i_f)\cos(\Delta\Omega) \tag{4}$$

$$\cos(i) = \cos(i_f)\cos(i^*) - \cos(\omega_f + \Omega^*)\sin(i_f)\sin(i^*) \tag{5}$$

$$\frac{\sin(i^*)}{\sin(\Delta\Omega)} = \frac{\sin(i)}{\sin(\omega_f + \Omega^*)} \tag{6}$$

where $\Delta\Omega = \Omega_f - \Omega$; Ω^* is the RAAN asociated to the target orbit reference frame; and i_f, Ω_f, and ω_f are the inclination, RAAN, and argument of perigee of the target orbit, respectively.

Regarding the second task, as γ quantifies the rate of change of i^* strictly produced by the RAAN drift of the current and target orbits, the subsequent chain rule can be applied:

$$\gamma = \left.\frac{\mathrm{d}i^*}{\mathrm{d}t}\right|_{J_2} = \frac{\partial i^*}{\partial \Delta\Omega}\frac{\mathrm{d}\Delta\Omega}{\mathrm{d}t} \tag{7}$$

Taking the corresponding partial derivative of Eq. (4) and substituting Eq. (6) yields:

$$\frac{\partial i^*}{\partial \Delta\Omega} = \sin(i_f)\sin(\omega_f + \Omega^*) \tag{8}$$

In turn, subtracting the RAAN drifts experimented by the target and the current orbits (Eq. (3)) and substituting Eq. (5) results in:

$$\frac{\mathrm{d}\Delta\Omega}{\mathrm{d}t} = -\frac{3}{2}R_\oplus^2 J_2\left(\sqrt{\frac{\mu}{a_f^7}}\cos(i_f) - \sqrt{\frac{\mu}{a^7}}\left(\cos(i_f)\cos(i^*) - \cos(\omega_f + \Omega^*)\sin(i_f)\sin(i^*)\right)\right) \tag{9}$$

It has to be noted that the term $(\omega_f + \Omega^*)$ appears in the definition of γ, but the differential equation that describes its temporal evolution is not considered in the problem dynamics. Therefore, given the value of γ at a certain epoch, the propagation of Eqs. (1,2) is not enough to determine its value at future time instants. Fortunately, the following properties of the considered transfer can be exploited to propagate γ without the need for adding an additional differential equation to the problem dynamics:

1) i is modified exclusively by the thrust.
2) $(\omega_f + \Omega^*)$ is modified exclusively by the J_2 perturbation.
3) $\Delta\Omega$ is modified by both the thrust and the J_2 perturbation.

Thus, given the values of all the variables up to a certain point in time, the propagation to a subsequent epoch can be performed as follows:

1) The values of a and i^* can be obtained with a straightforward propagation of Eqs. (1,2).
2) When considering Keplerian dynamics, $(\omega_f + \Omega^*)$ remains constant, while the obtained i would be identical to the one of the J_2-perturbed case. Consequently, computing i^* for the Keplerian case (i.e., $\gamma = 0$) and introducing it, together with $(\omega_f + \Omega^*)$, into Eq. (5) would result in the desired value of i.
3) The Keplerian value of $\Delta\Omega$ results from substituting the Keplerian values of i, $(\omega_f + \Omega^*)$, and i^* in Eqs. (4,6).

Then, its corresponding nodal precession (Eq. (3)) can be added to obtain its J_2-perturbed counterpart.

4) Subsequently, the J_2-perturbed value of $(\omega_f + \Omega^*)$ results from Eqs. (5,6).

5) Finally, Eq. (7) is used to compute γ.

B. Optimality conditions

The optimal control formulation of the problem at hand involves the minimization of the transfer time, as depicted in the following objective function:

$$J = \min \int_{t_0}^{t_f} \mathrm{d}t \tag{10}$$

where t_0 is the fixed initial time and t_f is a free final time.

Subject to the dynamics defined by Eqs. (1,2) and the following boundary conditions:

$$\begin{aligned} a(t_0) &= a_0 \quad i^*(t_0) = i_0^* \\ a(t_f) &= a_f \quad i^*(t_f) = 0 \end{aligned} \tag{11}$$

where a_0 and a_f are the initial and final values of the semimajor axis, respectively, and i_0^* is the initial relative inclination.

The Pontryagin's minimum principle states that the optimal solution of this problem requires the selection of a control law of β such that the following Hamiltonian function is minimized throughout the whole optimal trajectory:

$$\mathcal{H} = 1 + \lambda_a \left(2\sqrt{\frac{a^3}{\mu}} f \cos(\beta) \right) + \lambda_i \left(\frac{2}{\pi} \sqrt{\frac{a}{\mu}} f \sin(\beta) + \gamma \right) \tag{12}$$

where λ_a and λ_i are the costate variables associated to Eqs. (1,2), respectively. The following differential equations determine the rates of change of the costate variables:

$$\frac{\mathrm{d}\lambda_a}{\mathrm{d}t} = -\frac{\partial \mathcal{H}}{\partial a} = -\frac{f}{\sqrt{\mu}} \left(3\lambda_a \sqrt{a} \cos(\beta) + \frac{\lambda_i}{\pi\sqrt{a}} \sin(\beta) \right) - \lambda_i \frac{\partial \gamma}{\partial a} \tag{13}$$

$$\frac{\mathrm{d}\lambda_i}{\mathrm{d}t} = -\frac{\partial \mathcal{H}}{\partial i^*} = -\lambda_i \frac{\partial \gamma}{\partial i^*} \tag{14}$$

The necessary condition for the Hamiltonian function minimization is:

$$\frac{\partial \mathcal{H}}{\partial \beta} = -2\lambda_a \sqrt{\frac{a^3}{\mu}} f \sin(\beta) + \frac{2}{\pi} \lambda_i \sqrt{\frac{a}{\mu}} f \cos(\beta) = 0 \tag{15}$$

Resulting in the following optimal control law:

$$\tan(\beta) = \frac{\lambda_i}{\lambda_a \pi a} \tag{16}$$

It has to be noted that time does not explicitly appear in the Hamiltonian function (Eq. (12)). Hence, its value is constant throughout the whole optimal trajectory. Furthermore, t_f is a free variable and its associated boundary conditions are time-independent. Consequently, $\mathcal{H}(t_f) = 0$ and, by extension, is null during the whole trajectory. This condition, along with the optimal control law (Eq. (16)), can be used to unambiguously define the sine and cosine of β as functions of the costate variables:

$$\sin(\beta) = -\frac{2\lambda_i \sqrt{a} f}{\pi \sqrt{\mu}\,(1 + \lambda_i \gamma)} \tag{17}$$

$$\cos(\beta) = -\frac{2\lambda_a \sqrt{a^3} f}{\sqrt{\mu}\,(1 + \lambda_i \gamma)} \tag{18}$$

The costate variables can be also given as functions of β as follows:

$$\lambda_i = -\frac{\sin(\beta)}{\frac{2}{\pi}\sqrt{\frac{a}{\mu}} f + \gamma \sin(\beta)} \tag{19}$$

$$\lambda_a = -\frac{\cos(\beta)}{2\sqrt{\frac{a^3}{\mu}} f + \gamma \pi a \sin(\beta)} \tag{20}$$

Finally, the strong Legendre–Clebsch condition guarantees that a local minimum is obtained (as opposed to a maximum or saddle point).

$$\frac{\partial^2 \mathcal{H}}{\partial \beta^2} = -2\lambda_a \sqrt{\frac{a^3}{\mu}} f \cos(\beta) - \frac{2}{\pi} \lambda_i \sqrt{\frac{a}{\mu}} f \sin(\beta) > 0 \tag{21}$$

Adding Eq. (12) yields:

$$\lambda_i \gamma > -1 \tag{22}$$

Then, substituting λ_i from Eq. (19) gives:

$$\frac{\gamma \sin(\beta)}{\frac{2}{\pi}\sqrt{\frac{a}{\mu}} f + \gamma \sin(\beta)} < 1 \tag{23}$$

This expression implies that the signs of its denominator and the first term of such denominator have to be identical. By definition, said first term is positive. Hence, the following condition is sufficient for the obtention of a local minimum:

$$\frac{2}{\pi}\sqrt{\frac{a}{\mu}}f + \gamma \sin(\beta) > 0 \tag{24}$$

C. Heuristic control laws

When focusing on the computational efficiency of the resolution of optimal control problems, it is worth to investigate promising heuristic control laws. Specifically, control laws independent of the costates that, albeit suboptimal, can achieve near-optimal solutions under the right circumstances. This way, such near-optimal solutions can be obtained by simply propagating the state equations to the desired final state. Two promising heuristics are subsequently presented, namely, the proportional control law and the corrected Edelbaum strategy.

The selection of β involves a trade-off between the magnitude of the in-plane (to modify a) and out-of-plane (to change i^*) thrust components. The proportional control law allocates the thrust components such that the rates of change of the state variables are proportional to their difference with the target values, that is:

$$\frac{\mathrm{d}a/\mathrm{d}t}{\mathrm{d}i^*/\mathrm{d}t} = -\frac{a_f - a}{i^*} \tag{25}$$

For the sake of simplicity, Eq. (25) is reformulated as follows:

$$\frac{\phi_a \cos(\beta)}{\phi_i \sin(\beta) + \gamma} = d \tag{26}$$

where d is the right hand side of Eq. (25) and ϕ_a, ϕ_i are the factors that multiply $\cos(\beta)$, $\sin(\beta)$ in Eqs. (1,2), respectively.

Using the Pythagorean trigonometric identity, the sine and cosine of β can be isolated. This results in two possible solutions of Eq. (26). Nevertheless, one of those solutions increases the gap between both of the current states and the target orbit, while the other solution does the opposite. Thus, the only relevant solution is:

$$\sin(\beta) = -\frac{\phi_i \gamma d^2 + \phi_a \sqrt{\phi_a^2 + (\phi_i^2 - \gamma^2)d^2}}{\phi_a^2 + \phi_i^2 d^2} \tag{27}$$

$$\cos(\beta) = \frac{d\left(\phi_a \gamma - \phi_i \sqrt{\phi_a^2 + (\phi_i^2 - \gamma^2)d^2}\right)}{\phi_a^2 + \phi_i^2 d^2} \tag{28}$$

In turn, the corrected Edelbaum control law straightforwardly considers the β of the Edelbaum analytical solution.

$$\beta = \mathrm{atan2}\left(-\sin\left(\frac{\pi}{2}i^*\right), \sqrt{\frac{a_f}{a}} - \cos\left(\frac{\pi}{2}i^*\right)\right) \tag{29}$$

However, as this control law ignores the effect of the J_2 perturbation, the expected terminal state will not be exactly achieved. This problem is ameliorated by using the proportional control law during the last revolution of the transfer. Hence the name of corrected Edelbaum strategy.

D. Problem resolution

In general, the resolution of the problem at hand involves the propagation of the dynamics differential equations (Eqs. (1,2,13,14)), while fulfilling the optimal control law (Eqs. (17,18)). Moreover, the accomplishment of the desired boundary conditions at t_f (Eq. (11)) requires the determination of specific initial values for the costate variables. This can prove difficult because such variables do not possess a clear physical meaning. Nevertheless, in this particular case, Eqs. (19,20) provide the values of such costates as a function of β. Therefore, the boundary conditions at t_f can be achieved by simply selecting a suitable initial value of β, which has a bounded domain as well as a straightforward meaning. Consequently, the whole resolution process can be encapsulated in the following scalar univariate shooting function:

$$\psi : \beta(t_0) \rightarrow a(t_f) - a_f \tag{30}$$

Given an initial value of β, the shooting function propagates the dynamics equations until $i^* = 0$ and returns the defect of the resulting semimajor axis at that epoch, i.e., t_f. Hence, a root of ψ generates an optimal trajectory that complies with the boundary conditions. The following two-stage approach has been devised to obtain the aforementioned root:

1) The initial β angles corresponding to the proportional and corrected Edelbaum heuristic control laws are used to initialize a secant method. This method is executed until two values of ψ with different signs are found or until the solution is obtained, whichever happens first.
2) If the solution has not been obtained during the previous stage, the β angles corresponding to the values of ψ with different signs are used to execute Brent's bracketing method [14]. This way, the convergence to an optimal solution is guaranteed (assuming that ψ is continuous).

III. Three-arc transfer

When dealing with transfers involving a significant $\Delta\Omega$, continuous-thrust maneuvers may require an infeasible amount of Δv. In those cases, it is interesting to exploit the RAAN drift produced by the J_2 perturbation. Specifically, the usual strategy is to introduce an intermediate coasting arc in which the satellite will remain in a drifting orbit with an advantageous nodal precession.

A. SES strategy

The previously mentioned SES strategy [9] comprises two propulsive arcs, modelled with the Edelbaum solution, split apart by a coasting arc. This way, the propulsive arcs simultaneously modify a and i, while the whole $\Delta\Omega$ is overcome exclusively by the J_2 perturbation. Therefore, defining $\Delta v_{\text{Ed}}(a_0, i_0, a_1, i_1)$ as the Δv consumed during an Edelbaum transfer from (a_0, i_0) to (a_1, i_1), the Δv spent during the whole maneuver is:

$$\Delta v = \Delta v_{\text{Ed}}(a_0, i_0, a_0 + \Delta a, i_0 + \Delta i) + \Delta v_{\text{Ed}}(a_0 + \Delta a, i_0 + \Delta i, a_f, i_f) \tag{31}$$

where Δa and Δi are the necessary parameter variations to reach the drifting orbit. In turn, the Δt spent during this maneuver is:

$$\Delta t = \frac{\Delta v}{f} + t_{\text{drift}} \tag{32}$$

where t_{drift} is the drifting time, whose value is unambiguously determined by the fact that a RAAN difference of $\Delta\Omega$ has to be crossed over during the transfer. That is:

$$t_{\text{drift}} = -\frac{\Delta\Omega + \Delta(\Delta\Omega_1) + \Delta(\Delta\Omega_2)}{\Delta\dot{\Omega}_{\text{drift}}} \tag{33}$$

where $\Delta(\Delta\Omega_1)$ and $\Delta(\Delta\Omega_2)$ are the variations of $\Delta\Omega$ due to the J_2 perturbation during the first and second propulsive arcs, respectively, and $\Delta\dot{\Omega}_{\text{drift}}$ is the rate of change of $\Delta\Omega$ during the coasting arc. Both $\Delta(\Delta\Omega_1)$ and $\Delta(\Delta\Omega_2)$ are computed through a numerical integration of Eq. (3).

Eqs. (31,32) can be used to formulate a rather manageable single-constraint NLP problem of two variables (i.e., Δa and Δi). Hence the efficiency and reliability of this method.

B. Relative Inclination Change (RIC) strategy

The SES strategy proves especially Δv-efficient when the available time to perform a transfer is such that the whole $\Delta\Omega$ can be traversed with moderate variations of the RAAN drift. However, when considering stingier transfer times, it is notably advantageous to use the thrust to also modify the RAAN [10]. This concept can be exploited by substituting the second Edelbaum propulsive arc with the relative inclination change maneuver described in Section II. Hence, this approach is expected to outperform the SES strategy for tight transfer times. In turn, for longer transfer times both approaches are nearly identical, the difference being that the RIC strategy inevitably performs a small $\Delta\Omega$ change. Therefore, this approach is expected to be slightly worse than the SES strategy for such transfer times.

Defining $\Delta v_{\text{RIC}}(a_0, i_0, a_1, i_1, \Delta\Omega_0)$ as the Δv consumed during a relative inclination change transfer from (a_0, i_0) to (a_1, i_1) with an initial RAAN difference of $\Delta\Omega_0$; the Δv spent during the whole maneuver is:

$$\Delta v = \Delta v_{\mathrm{Ed}}(a_0, i_0, a_0 + \Delta a, i_0 + \Delta i) + \Delta v_{\mathrm{RIC}}(a_0 + \Delta a, i_0 + \Delta i, a_f, i_f, \Delta\Omega_0 + \Delta\Delta\Omega_1 + \Delta\dot{\Omega}_{\mathrm{drift}} t_{\mathrm{drift}}) \tag{34}$$

The Δt spent during this maneuver is also defined by Eq. (32). However, as the second propulsive arc is able to modify $\Delta\Omega$, t_{drift} is a variable to be determined during the optimization. Thus, Eqs. (32,34) result in a NLP problem of three variables (i.e., Δa, Δi, and t_{drift}).

IV. Results

Numerical experiments have been performed to provide a comparison between the RIC strategy and other relevant methodologies. In decreasing order of complexity, the considered approaches can be classified into optimal control problems (YSS [10], Cerf [9]), NLP problems (RIC, SES [9]), and analytical approximations (Shen [13]).

Specifically, the RIC and SES strategies are used to numerically solve a set of test cases, which involve the minimization of the Δv spent during a transfer while complying with a maximum transfer time. Such tests cases are depicted in Table 1,

Table 1 Test cases

Case	Δt_{max} (days)	$\Delta\Omega_0$ (deg)	h_0 (km)	h_f (km)	i_0 (deg)	i_f (deg)
1	100	30	800	900	98	99
2	10	3	800	900	98	99
3	100	10	800	900	98	99
4	24.86	0.46	779.3	733.8	98.64	97.45

where h_0 and h_f are the initial and final orbital altitudes, respectively, and Δt_{max} is the maximum transfer time. Cases 1 and 2 have been extracted from Ref. [10], while Cases 3 and 4 have been obtained from Ref. [13]. The values of the constants of the gravitational model used during the resolution of the test cases are: $J_2 = 1.082635854 \cdot 10^{-3}$, $\mu = 3.986004418 \cdot 10^{14}$ m^{3}s^{-2}, and $R_\oplus = 6378137$ m.

Tables 2 and 3 show the Δv consumed by the RIC and SES strategies for the aforementioned test cases, as well as the solutions achieved by other methods provided in the literature.

Table 2 Method performance comparison (Test cases 1 and 2)

	Case 1	Case 2
Method	Δv (ms^{-1})	Δv (ms^{-1})
YSS [10]	596.7	507.0
Cerf [9]	598.1	652.5
SES [9]	598.2	664.3
RIC	598.8	567.2

The comparison of the RIC strategy with the other relevant methods can be summarized as follows:

Table 3 Method performance comparison (Test cases 3 and 4)

	Case 3	Case 4
Method	Δv (ms^{-1})	Δv (ms^{-1})
Shen (i) [13]	325.3	255.1
Shen (i,Ω) [13]	324.4	254.1
SES [9]	313.3	1187.6
RIC	313.5	245.0

1) SES: As anticipated in Section III.B, the RIC strategy clearly outperforms the SES strategy for tight transfer times (Cases 2 and 4), while being marginally worse for longer transfer times (Cases 1 and 3). As both methods have a similar computational complexity, it is reasonable to prefer the RIC strategy.
2) Cerf: The Cerf approach improves the Δv achieved by the SES strategy, at the cost of a greater computational complexity. However, when compared to the RIC strategy, it shows the same disadvantages as the SES strategy on top of the increased computational complexity.
3) YSS: The YSS method outperforms the RIC strategy. It is a logical result because the YSS method is a strict generalization of the RIC, SES and Cerf methods. However, due to the computational complexity of its associated optimal control problem, the YSS method might not be suitable for the formulation of large-scale combinatorial problems. Additionally, it has to be noted that several instances of the SES strategy are solved to obtain an initial guess of the costates of the YSS method. As the RIC strategy provides a Δv improvement over the SES strategy for longer transfer times, it might provide a better costate guess for those problem instances. Thus accelerating the resolution of the YSS method.
4) Shen: The RIC strategy outperforms both of Shen analytical approximations. Therefore, selection of which of these methods to use in a large-scale combinatorial problem involves a trade-off between solution quality and computational efficiency.

It has to be noted that the RIC strategy can make use of the heuristic control laws described in Section II.C to further accelerate the resolution of the method. Tables 4 and 5 show the Δv consumed for each of the control laws used during the second propulsive arc, as well as the Δa and Δi changes performed during the first propulsive arc.

Table 4 Heuristic control laws performance comparison (Test cases 1 and 2)

	Case 1			Case 2		
Method	Δv (ms^{-1})	Δa (km)	Δi (deg)	Δv (ms^{-1})	Δa (km)	Δi (deg)
Optimal	598.84	-391.77	1.216	567.23	-310.77	1.015
Corr. Edelbaum	599.05	-391.77	1.217	567.25	-310.77	1.014
Proportional	600.06	-375.60	1.294	567.78	-310.77	1.017

It can be seen that both heuristics achieve near-optimal solutions, with the corrected Edelbaum control law being

Table 5 Heuristic control laws performance comparison (Test cases 3 and 4)

	Case 3			Case 4		
Method	Δv (ms^{-1})	Δa (km)	Δi (deg)	Δv (ms^{-1})	Δa (km)	Δi (deg)
Optimal	313.46	-122.82	0.8957	245.03	-10.00	-0.3482
Corr. Edelbaum	313.46	-122.82	0.8957	245.03	-10.00	-0.3482
Proportional	313.46	-122.82	0.8957	245.04	-9.98	-0.3482

marginally better.

V. Conclusions

This manuscript proposes a novel J_2-perturbed continuous-thrust transfer between circular orbits. Specifically, this transfer considers tangential and out-of-plane thrust, with the thrust yaw angle being the sole control variable. Moreover, the dynamics of the transfer is described by two state variables. Namely, the semimajor axis and the relative inclination w.r.t. the target orbit. The optimal solution of this problem involves finding a root of a function of the thrust yaw angle. Two heuristic control laws provide initial guesses for this root-finding problem. The convergence of this solution can be guaranteed with the use of bracketing root-finding methods, assuming that the function is continuous.

Furthermore, a thrust-coast-thrust strategy has been formulated. Its first propulsive arc corresponds to an Edelbaum transfer, while the second one performs the aforementioned relative inclination change transfer. This results in a three-variable NLP problem. The performance of this strategy for time-constrainted Δv-optimal transfers has been compared with the solutions of other relevant methods of the literature. It has been shown that the proposed three-arc strategy provides an advantageous trade-off between solution quality and computational complexity. Thus being suitable for the formulation of large-scale combinatorial problems. Finally, it has been shown that the use of the proposed heuristic control laws in the second propulsive arc results in near-optimal solutions, while further accelerating the resolution process.

Acknowledgments

AB and HU wish to acknowledge funding from grant PID2020-112576GB-C22 of the Spanish State Research Agency and the European Regional Development Fund. AB also wishes to acknowledge funding from grant PREDOC20-003 of “Universidad Rey Juan Carlos”. LC wishes to acknowledge support from Project Grant F663 - AAGNCS by the “Dirección General de Investigación e Innovación Tecnológica, Consejería de Ciencia, Universidades e Innovación, Comunidad de Madrid” and “Universidad Rey Juan Carlos”.

References

[1] Kessler, D. J., and Courpalais, B. G., "Collision Frequency of Artificial Satellites - Creation of a Debris Belt," *Journal of Geophysical Research-Space Physics*, Vol. 83, No. NA6, 1978, pp. 2637–2646. https://doi.org/10.1029/JA083iA06p02637.

[2] Liou, J.-C., and Johnson, N. L., "A sensitivity study of the effectiveness of active debris removal in LEO," *Acta Astronautica*, Vol. 64, No. 2-3, 2009, pp. 236–243. https://doi.org/10.1016/j.actaastro.2008.07.009.

[3] Lewis, H. G., White, A. E., Crowther, R., and Stokes, H., "Synergy of debris mitigation and removal," *Acta Astronautica*, Vol. 81, 2012, pp. 62–68. https://doi.org/10.1016/j.actaastro.2012.06.012.

[4] Edelbaum, T. N., "Propulsion requirements for controllable satellites," *Ars Journal*, Vol. 31, No. 8, 1961, pp. 1079–1089. https://doi.org/10.2514/8.5723.

[5] Kechichian, J. A., "Reformulation of Edelbaum's low-thrust transfer problem using optimal control theory," *Journal of Guidance, Control, and Dynamics*, Vol. 20, No. 5, 1997, pp. 988–994. https://doi.org/10.2514/2.4145.

[6] Casalino, L., and Colasurdo, G., "Improved Edelbaum's approach to optimize low earth/geostationary orbits low-thrust transfers," *Journal of guidance, control, and dynamics*, Vol. 30, No. 5, 2007, pp. 1504–1511. https://doi.org/10.2514/1.28694.

[7] Kluever, C. A., "Using edelbaum's method to compute Low-Thrust transfers with earth-shadow eclipses," *Journal of Guidance, Control, and Dynamics*, Vol. 34, No. 1, 2011, pp. 300–303. https://doi.org/10.2514/1.51024.

[8] Gatto, G., and Casalino, L., "Fast evaluation and optimization of low-thrust transfers to multiple targets," *Journal of Guidance, Control, and Dynamics*, Vol. 38, No. 8, 2015, pp. 1525–1530. https://doi.org/10.2514/1.G001116.

[9] Cerf, M., "Low-thrust transfer between circular orbits using natural precession," *Journal of Guidance, Control, and Dynamics*, Vol. 39, No. 10, 2016, pp. 2232–2239. https://doi.org/10.2514/1.G001331.

[10] Wen, C., Zhang, C., Cheng, Y., and Qiao, D., "Low-Thrust Transfer Between Circular Orbits Using Natural Precession and Yaw Switch Steering," *Journal of Guidance, Control, and Dynamics*, 2021, pp. 1–8. https://doi.org/10.2514/1.G005790.

[11] Li, H., Chen, S., and Baoyin, H., "J2-perturbed multitarget rendezvous optimization with low thrust," *Journal of Guidance, Control, and Dynamics*, Vol. 41, No. 3, 2018, pp. 802–808. https://doi.org/10.2514/1.G002889.

[12] Barea, A., Urrutxua, H., and Cadarso, L., "Large-scale object selection and trajectory planning for multi-target space debris removal missions," *Acta Astronautica*, Vol. 170, 2020, pp. 289–301. https://doi.org/10.1016/j.actaastro.2020.01.032.

[13] Shen, H.-X., "Explicit Approximation for J 2-Perturbed Low-Thrust Transfers Between Circular Orbits," *Journal of Guidance, Control, and Dynamics*, 2021, pp. 1–7. https://doi.org/10.2514/1.G005415.

[14] Brent, R. P., *An Algorithm with Guaranteed Convergence for Finding a Zero of a Function*, Algorithms for minimization without derivatives, Prentice-Hall, Englewood Cliffs, NJ, 1973, pp. 47–58. https://doi.org/10.1093/comjnl/14.4.422.